AD-A195 332 CRYSTALLINITY OF RF-SPUTTERED MOS2 FILMS(U) AEROSPACE 1/1
CORP EL SEGUNDO CA CHEMISTRY AND PHYSICS LAB
J R LINCE ET AL. 15 APR 88 TR-0086A(2945-03)-2
UNCLASSIFIED SD-TR-88-26 F04701-85-C-0086 F/G 11/6.2 NL

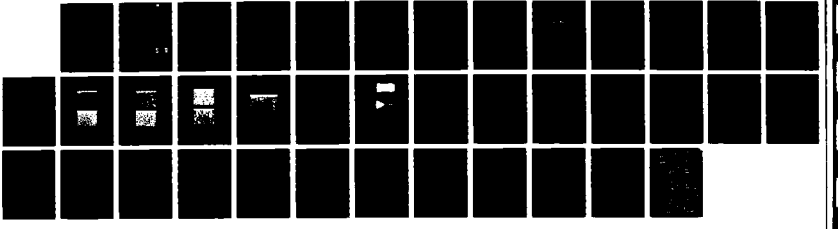

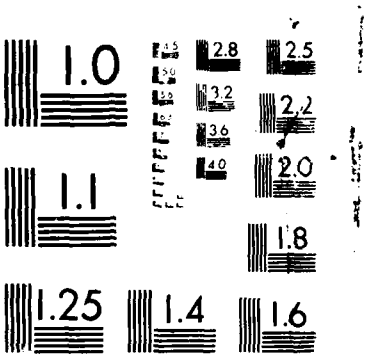

REPORT SD-TR-88-26

Crystallinity of RF-Sputtered MoS_2 Films

J. R. LINCE and PAUL D. FLEISCHAUER
Chemistry and Physics Laboratory
Laboratory Operations
The Aerospace Corporation
El Segundo, CA 90245

15 April 1988

Prepared for

SPACE DIVISION
AIR FORCE SYSTEMS COMMAND
Los Angeles Air Force Base
P.O. Box 92960, Worldway Postal Center
Los Angeles, CA 90009-2960

UNCLASSIFIED

SECURITY CLASSIFICATION OF THIS PAGE

REPORT DOCUMENTATION PAGE

1a. REPORT SECURITY CLASSIFICATION Unclassified	1b. RESTRICTIVE MARKINGS
2a. SECURITY CLASSIFICATION AUTHORITY	3. DISTRIBUTION / AVAILABILITY OF REPORT Approved for public release; distribution unlimited.
2b. DECLASSIFICATION / DOWNGRADING SCHEDULE	
4. PERFORMING ORGANIZATION REPORT NUMBER(S) TR-0086A(2945-03)-2	5. MONITORING ORGANIZATION REPORT NUMBER(S) SD-TR-88-26
6a. NAME OF PERFORMING ORGANIZATION The Aerospace Corporation Laboratory Operations 6b. OFFICE SYMBOL (If applicable)	7a. NAME OF MONITORING ORGANIZATION Space Division
6c. ADDRESS (City, State, and ZIP Code) El Segundo, CA 90245	7b. ADDRESS (City, State, and ZIP Code) Los Angeles Air Force Base Los Angeles, CA 90009-2960
8a. NAME OF FUNDING / SPONSORING ORGANIZATION 8b. OFFICE SYMBOL (If applicable)	9. PROCUREMENT INSTRUMENT IDENTIFICATION NUMBER F04701-85-C-0086-P00016
8c. ADDRESS (City, State, and ZIP Code)	10. SOURCE OF FUNDING NUMBERS PROGRAM ELEMENT NO. / PROJECT NO. / TASK NO. / WORK UNIT ACCESSION NO.

11. TITLE (Include Security Classification)

Crystallinity of RF-Sputtered MoS_2 Films

12. PERSONAL AUTHOR(S)

Lince, Jeffrey R., and Fleischauer, Paul D.

13a. TYPE OF REPORT	13b. TIME COVERED FROM _____ TO _____	14. DATE OF REPORT (Year, Month, Day)	15. PAGE COUNT
		1988 April 15	34

16. SUPPLEMENTARY NOTATION

17. COSATI CODES		
FIELD	GROUP	SUB-GROUP

18. SUBJECT TERMS (Continue on reverse if necessary and identify by block number)

Solid lubricant films; Thin-film stress; Molybdenum disulfide; Lattice defects; Radio-frequency sputtering; X-ray diffraction

19. ABSTRACT (Continue on reverse if necessary and identify by block number)

The crystallinity and morphology of thin, radio-frequency (rf)-sputtered MoS_2 films deposited on 440C stainless steel substrates at both ambient (≤ 70°C) and high temperatures (245°C) were studied by scanning electron microscopy (SEM) and by x-ray diffraction (Read thin-film photography and θ-2θ scans). Under SEM, the films exhibited a "ridgelike" (or platelike) formation region for thicknesses between 0.18 and 1.0 μm MoS_2. X-ray diffraction was shown to give more detailed and accurate information than electron diffraction previously used for elucidating the structure of sputtered lubricant films. Read thin-film x-ray diffraction photographs revealed patterns consistent with the presence of polycrystalline

20. DISTRIBUTION / AVAILABILITY OF ABSTRACT	21. ABSTRACT SECURITY CLASSIFICATION
☐ UNCLASSIFIED/UNLIMITED ☒ SAME AS RPT. ☐ DTIC USERS	Unclassified
22a. NAME OF RESPONSIBLE INDIVIDUAL	22b. TELEPHONE (Include Area Code) / 22c. OFFICE SYMBOL

DD FORM 1473, 84 MAR 83 APR edition may be used until exhausted. All other editions are obsolete.

SECURITY CLASSIFICATION OF THIS PAGE

UNCLASSIFIED

18. SUBJECT TERMS (Continued)

Scanning electron microscopy
Thin-film morphology
Crystallite orientation
Friction and wear behavior

19. ABSTRACT (Continued)

films and strong orientation of the MoS_2 crystallites. Correlation of those patterns with θ-2θ scans of the films indicated that the basal planes of the MoS_2 crystallites [i.e., the (0 0 1) planes] were perpendicular to the substrate surface plane, and that various edge planes [i.e., the (h k 0) planes] in the individual crystallites were parallel to the surface plane, in agreement with previous observations of thinner films. Sliding wear caused the crystallites to orient with their basal planes parallel to the surface plane. The crystallite lattices in all films in this study were shown to exhibit compressive stress (~ 3%-5% with respect to natural molybdenite) in the direction perpendicular to the (h k 0) planes, and the worn films were expanded (i.e., exhibited tensile stress) perpendicular to the (0 0 1) plane. In addition, the shapes of the x-ray diffraction peaks were strongly influenced by the presence of oxygen impurities and/or sulfur vacancies in the MoS_2 lattice, indicating that x-ray diffraction may provide a simple quality-control test for the production of a film with optimum lubricating properties.

PREFACE

The authors thank Reinhold Bauer for instruction in the use of the sputtering chamber, for sharing some of his x-ray diffraction data, and for numerous helpful discussions; Paul Adams for taking the x-ray diffraction data and for providing helpful comments; and Michael Gardos and Russell Lipeles for helpful discussions.

CONTENTS

FIGURES

TABLE

I. INTRODUCTION

The current approach to optimizing the friction and wear characteristics of solid lubricant films is empirical. For example, parameters used in the radio-frequency (rf)-sputtering process to produce MoS_2 films are varied until the "best" films are obtained, but the way in which changes in the basic chemical and physical properties of those films affect their wear behavior is not well understood. Better understanding of these properties will enable production of films that exhibit "absolute" rather than "relatively" optimal wear behavior with respect to variation of their chemical and physical structure parameters.

The low coefficient of friction of MoS_2 results directly from its hexagonal, two-dimensional crystal structure (see Fig. 1); hence, the crystallinity of rf-sputtered MoS_2 films should be highly correlated with their lubrication properties. Cleaving an MoS_2 single crystal to produce a basal plane (0 0 1) surface does not result in the breaking of covalent bonds, because successive basal planes are bonded to each other by relatively weak van der Waals forces. Therefore, cleavage results in the production of a highly inert surface with no dangling bonds.

The wear life of a solid lubricant film is dependent on the adhesion of the film to a lubricated device. The adhesion can be shown to be related to, among other factors, the stress within the film.[1] Films grown by high-rate techniques, such as rf sputtering, generally exhibit significant amounts of stress.[2] Therefore, it is advantageous to develop methods of detecting stress within rf-sputtered films in order to correlate the stress with the film's wear behavior.

Until now, there have been few studies of the crystallinity and stress within sputtered MoS_2 films, although the basic morphology of the films has been well studied by electron microscopy. Spalvins[3] used transmission electron microscopy and diffraction (TEM) and (TED) to show that very thin (~ 400 Å) rf-sputtered films have crystallites oriented with their edge planes [i.e., (h k 0)-type planes] parallel to the substrate surface. He also

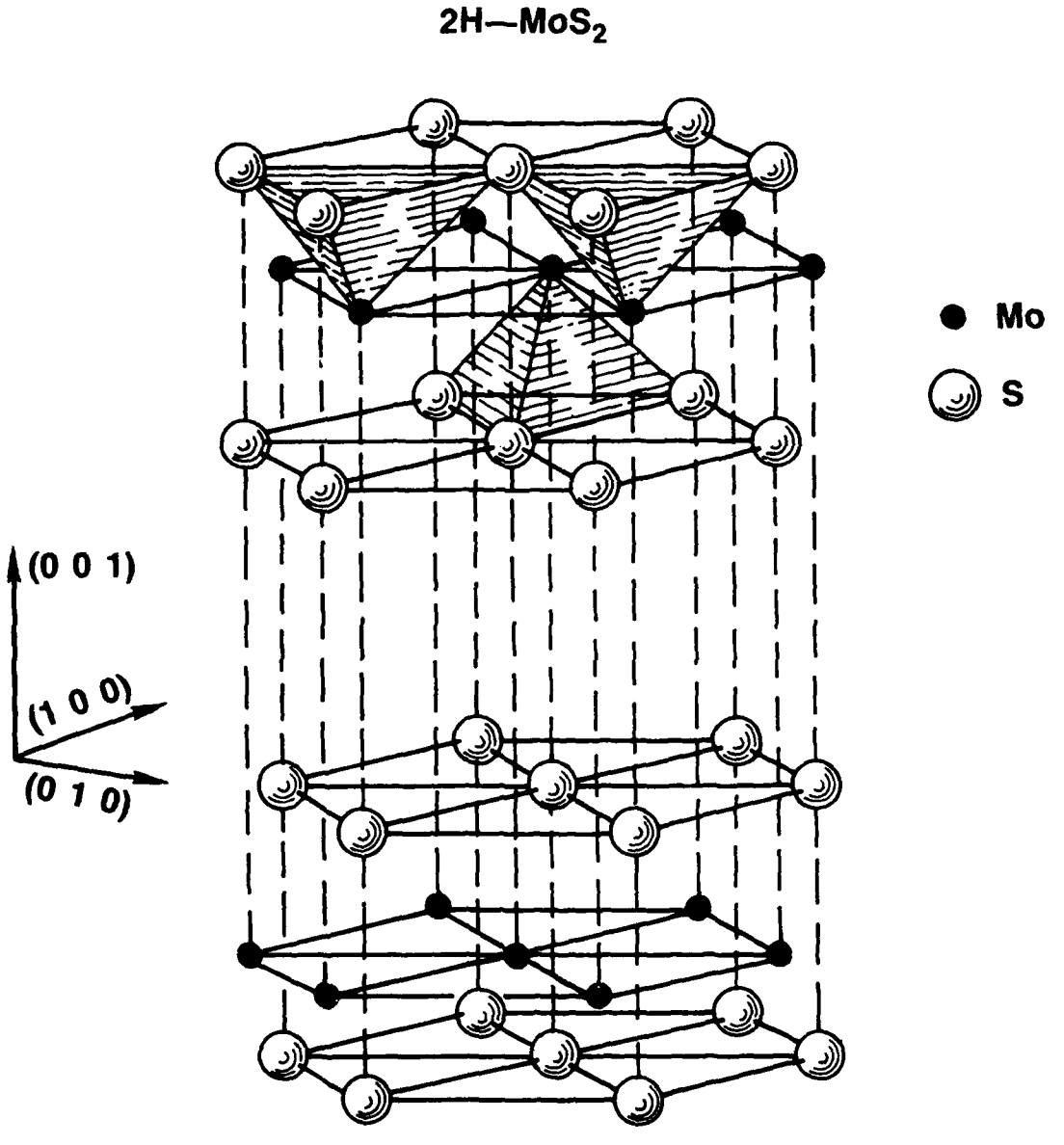

Fig. 1. Molybdenum disulfide (MoS_2) crystal structure.

suggested that a measurement of the widths of the diffraction rings gives a qualitative measure of the size of the crystallites. Dimigen and coworkers[4] used TED to examine material that had been removed from substrates on which MoS_x films had been deposited. They demonstrated that the basic MoS_2 crystal structure was retained, even for highly sulfur-deficient films, i.e., for $1.0 \leq x < 2.0$.

TED, however, has a number of disadvantages. Reliable lattice constant information is difficult to obtain: Spectra of intensity vs electron scattering angle are not normally obtained with TED, making it impossible to examine line profiles in detail. Also, its major limitation for analyzing the crystallinity of solid lubricant films is the difficulty of sample preparation. Because of the limited mean free path of electrons, only very thin films (i.e., $\lesssim$ 500 Å) can be examined, whereas commonly used lubricating film thicknesses are of the order of 5000 Å. TED also requires the substrate that the film is mounted on to be removed by dissolving it in an etch or by ion milling, or by depositing the film on a carbon film mounted on a specialized electron microscopy substrate.

X-ray diffraction[5] (XRD) offers three advantages over electron diffraction for the study of the crystallinity of thin solid lubricant films. First, the use of scintillation counters and highly accurate angle goniometers enables the x-ray line shape and position to be determined accurately so that the small shifts in lattice spacing (i.e., due to stress) may be discerned. Second, it can be performed on any substrate, as long as the positions of the substrate diffraction peaks do not interfere with the diffraction peaks of the film. Third, it is nondestructive, and can therefore be used to study crystalline changes after various stages of the wear process. A disadvantage of x-ray diffraction is that it requires more sample material than electron diffraction, because the extinction length of x rays (~ 10 000 Å) is considerably larger than the mean free path (~ 250 Å) of electrons. This disadvantage can be compensated for by using small x-ray incidence angles (i.e., grazing incidence) and/or longer counting times.

In the present study, x-ray diffraction is applied to the analysis of the crystallinity of rf-sputtered MoS_2 films on (mainly) 440C stainless steel substrates. We have used θ-2θ-type XRD scans and the Read thin-film camera XRD method to determine the degree of orientation and lattice spacings in the films. Details of the experimental procedure are discussed in Sec. II; the results are presented and discussed in terms of film chemistry and its possible effects on film tribology in Sec. III; and the conclusions are summarized in Sec. IV.

II. EXPERIMENTAL

The MoS_2 films were sputtered from a 152-mm (6-in.)-diameter target, manufactured by the Materials Research Corporation, that was made by hot-pressing MoS_2 powder (99.9% pure). The target was bonded to a water-cooled copper plate using a conductive epoxy before being mounted in the sputtering chamber. The substrates were 440C stainless steel with surface dimensions of 19 × 9.5 mm. They were polished with 0.3-μm Al_2O_3 powder in a slurry and degreased with acetone and methanol immediately before insertion into the sputtering chamber and subsequent pumpdown. The background pressure before sputtering was typically ~ 1×10^{-5} Torr.

The target was presputtered onto a shutter over the sample for 2 hr prior to film deposition in order to outgas the target and to permit the sputtering rate and stoichiometry to come to a steady state (i.e., a concentration ratio of S/Mo $\cong$ 2.0). During sputtering, the target-to-substrate distance was 36 mm, the argon sputtering gas pressure was ~ 2×10^{-2} Torr, and the power density was 1.93×10^4 W m^{-2}, resulting in typical sputtering rates of ~ 350-450 Å min^{-1}. The substrate was electrically grounded (i.e., had a bias voltage of 0 V). The substrates' temperatures either were allowed to float, which resulted in a substrate growth temperature of ~ 70°C (designated AT or ambient temperature) or were held at ~ 245°C (designated HT or high temperature) during sputtering. After sputtering, the chamber was vented with argon and the samples were placed in desiccators over anhydrous $CaSO_4$ until they could be analyzed by XRD. Some of the samples were annealed for various times at temperatures betweeen 200 and 500°C in a vacuum chamber with a base pressure of ~5×10^{-8} Torr before analysis. Representative samples were analyzed using a stylus-type surface profilometer to obtain nominal film thicknesses.

The MoS_2 films were analyzed by XRD within ~72 hr after sputter deposition: Previous studies in our laboratory using x-ray photoelectron spectroscopy (XPS) have shown that films exposed to atmosphere for this length of time have negligible postsputtering oxide formation.[6,7] The samples were analyzed using a Phillips Electronics APD-3720 vertical powder diffractometer

equipped for normal θ-2θ scans using Cu Kα x-rays (1.54-Å wavelength). They were oriented so that the scattering vector $\vec{G}$ (i.e., the vector subtraction of the incident x-ray vector from the outgoing x-ray vector) was always parallel to the surface normal. Some of the samples were analyzed by photographing the XRD pattern with a Read thin-film camera, for which the angle of incidence of the x rays (also Cu Kα) with respect to the substrate surface was 5°-15°, which serves to emphasize near-surface species in the XRD pattern. To separate the contribution of the film from that of the substrate in the x-ray pattern, single-crystal wafers of silicon were used as substrates for the Read thin-film photographs. The only pretreatment of the electronics-grade silicon wafers involved degreasing in acetone and methanol prior to sputtering MoS_2 on their surface, so it is assumed that a film of amorphous SiO_2 ~ 50 Å thick was present between the MoS_2 film and the single-crystal silicon. To investigate possible differences in film morphology, representative samples were subsequently analyzed by scanning electron microscopy (SEM) in a Cambridge Stereoscan S-200 scanning electron microscope.

Two of the films (on stainless steel substrates) were subjected to sliding wear in a test fixture described by Fleischauer and Bauer,[7] to determine changes in crystallinity during the wear process. The sliding contact was provided by a 440C stainless steel disk with a ~ 45.2-mm^2 area of contact and a 3.18-kg deadweight load on the samples. The speed of rotation was 123 rpm for an average sliding velocity of ~ 50 mm s^{-1}. The fixture could be filled with purified, extra-dry nitrogen gas and also contained $CaSO_4$ desiccant so that the ambient oxygen was very low and the measured humidity was ~ 0% during sliding wear.

III. RESULTS AND DISCUSSION

A. SCANNING ELECTRON MICROSCOPY OF MoS_2 FILMS

SEM photomicrographs of some of the films in this study are presented in Figs. 2 through 5. Although they are similar to SEM[8] and TEM[9] done by other researchers, they are presented here as references for our XRD data, because varying sputtering parameters between different studies can subtly affect the morphology of MoS_2 films. Both SEM photomicrographs shown in Fig. 2 are of AT 1-μm (~ 10 000 Å) thick films; however, the sample in Fig. 2(b) was annealed to 500°C for 1 hr after sputtering. The photomicrographs are quite similar when one takes into account the differences in contrast and focus. Both have the "wormlike" appearance that is generally observed for sputtered MoS_2 films and exhibit the typical dendrites that appear as small lines at approximate right angles to the sides of the larger particles. The SEM photomicrographs in Fig. 3 are for the same films as in Fig. 2, but were taken at higher magnification and with an off-normal electron incidence direction to emphasize structure perpendicular to the surface. They show that the MoS_2 particles are two dimensional (i.e., platelike) rather than one dimensional (i.e., wormlike). The only major difference between Figs. 3(a) and 3(b) is that there appear to be fewer dendrites in Fig. 3(a).

Two SEM photomicrographs of a 1-μm-thick HT film are presented in Fig. 4. The one in Fig. 4(a) was taken with the same magnification and electron incidence angle as in Fig. 2; the one in Fig. 4(b) was taken under the same conditions as in Fig. 3 and emphasizes the platelike structure of the film. There are obvious differences between the AT and HT films as manifested in the photomicrographs: The particles in the HT films are larger and farther apart than in the AT films, and the dendrites are completely absent for the HT films.

The SEM photomicrograph of an ~ 1800-Å-thick AT film, Fig. 5, was taken with the same magnification as in Fig. 2. That film appears to have the same basic structure as the thicker films (see Fig. 2), but the particles are somewhat smaller. The plate thickness (i.e., the thickness of the particle in

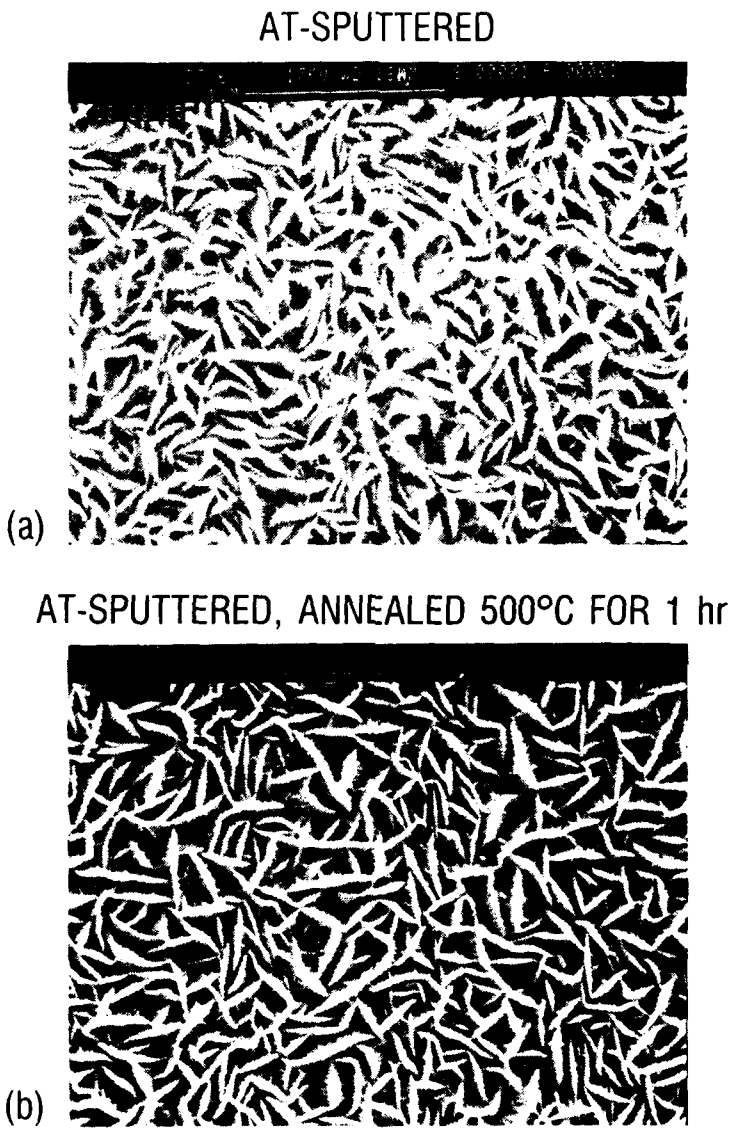

Fig. 2. SEM photomicrographs of 1-μm-thick MoS_2 films deposited on 440C stainless steel substrates held at ~ 70°C (AT films): (a) as prepared, and (b) annealed to 500°C for 1 hr. The electron beam was incident normal to the substrate surface. The magnification, electron energy, working distance, and length scale (1 μm) are noted on the photos.

AT-SPUTTERED, 35° OFF NORMAL

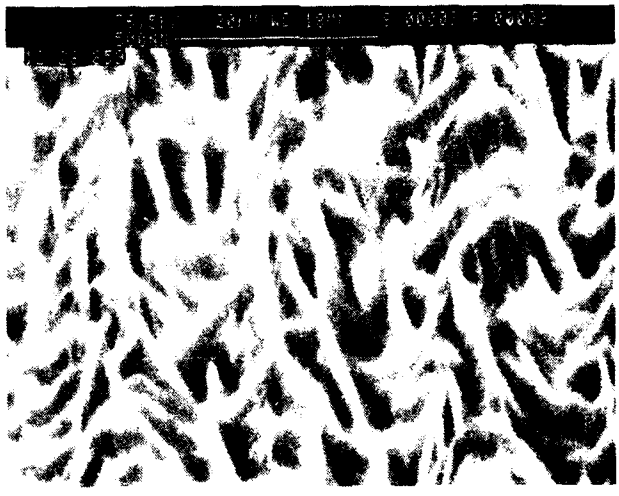

(a)

AT-SPUTTERED, ANNEALED 500°C FOR 1 hr, 35° OFF NORMAL

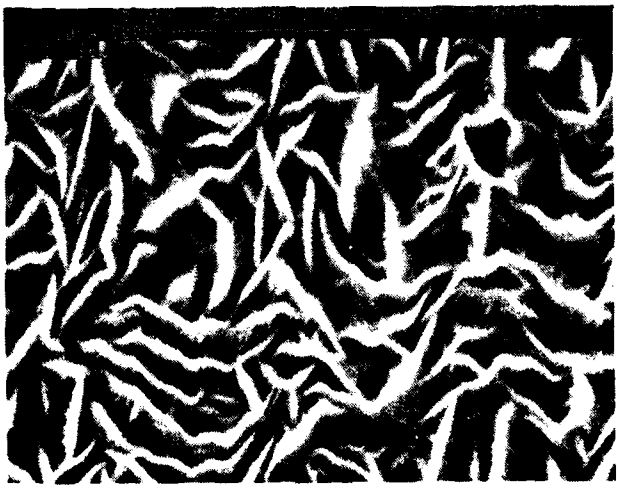

(b)

Fig. 3. SEM photomicrographs for the samples in Figs. 2(a) and 2(b), but with twice the magnification, and for an electron-beam incidence direction that is 35° from the substrate surface normal. The only apparent difference between the two photos is that in (b) there are slightly fewer dendrites. The differences in the appearance of (a) and (b) are mainly due to large differences in contrast between the two photos.

Fig. 4. SEM photomicrographs of a 1-μm-thick MoS_2 film deposited on a 440C stainless steel substrate held at 245°C (HT film). Electron-beam incidence direction: (a) 0° and (b) 35° from the surface normal. Photo (a) was taken with the same magnification as in Fig. 2, whereas (b) has twice that magnification.

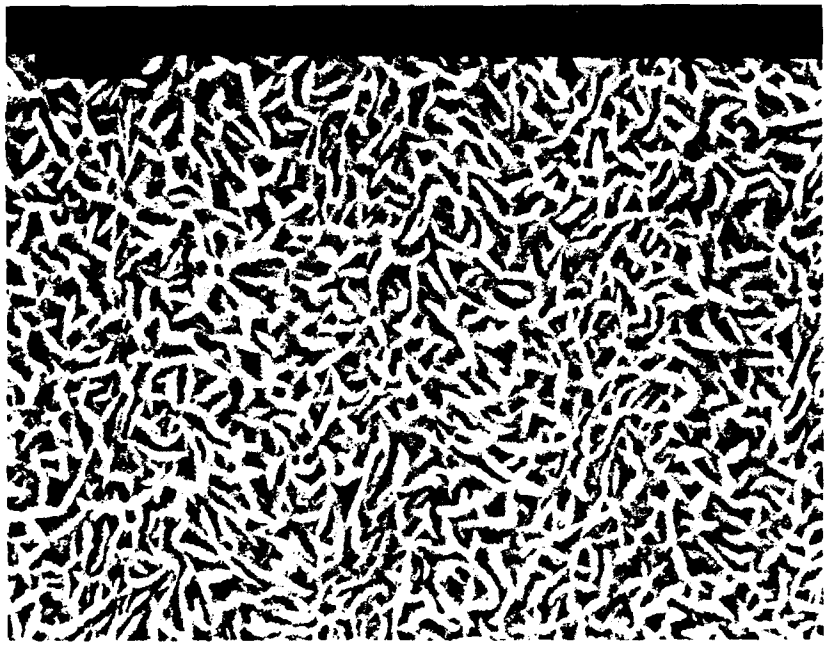

Fig. 5. SEM photomicrograph of an 1800-Å-thick AT MoS_2 film deposited on a 440C stainless steel substrate. The electron beam was incident normal to the substrate surface, and the magnification was the same as in Figs. 2 and 4(a).

the smallest dimension: ~ 300-400 Å) is approximately the same as that of the 1-μm-thick film. Other films studied in our laboratory that were intermediate in thickness between 0.18 and 1 μm exhibited the same basic structure as the 0.18- and 1.0-μm-thick films.

The film morphology as evident from the micrographs suggests that the films grow according to the following process: The particles (presumably crystallites) begin growing in three dimensions (although not isotropically) until they reach a certain thickness in the direction perpendicular to the (0 0 1) basal plane (i.e., ~ 300-400 Å); the particles then grow only perpendicular to the (h k 0) planes. In contrast, the mechanism proposed by Spalvins[9] is a three-step growth process in which an ~800-Å ridge region forms, followed by a ~ 2000-Å "equiaxed" region, and finally a columnar fiber structure that continues beyond 1-μm total thickness. The films in the present study appear to grow in the "ridge formation" (or platelike) region throughout the entire growth process, implying that the growth processes and morphologies of rf-sputtered MoS_2 films are sensitive to small changes in sputtering conditions, given the minimal differences between Spalvins' sputtering conditions and ours.

B. X-RAY DIFFRACTION OF MoS_2 FILMS USING READ THIN-FILM CAMERA

XRD patterns recorded with a Read camera should provide a qualitative distribution of the orientation of crystallites within a film, because such patterns include diffracted beams for which the scattering vector is not in the direction of the surface normal. Figure 6 presents Read thin-film photographs for a 1-μm-thick MoS_2 film that was sputtered onto a single-crystal silicon wafer prepared as described in Sec. II. The spots result from the silicon substrate, whereas the somewhat diffuse bands represent the MoS_2 film. In these photographs, the (1 0 0), (1 0 3), and (1 1 0) reflections are clearly visible; the (1 0 5) reflection is less visible. The line from point A to point B in Figs. 6(a) and 6(b) represents reflections for the scattering plane (the plane that contains the incident and scattered x rays) perpendicular to the sample surface, which is the same scattering plane as for θ-2θ scans. Note that Figs. 6(a) and 6(b) are of the same film but are

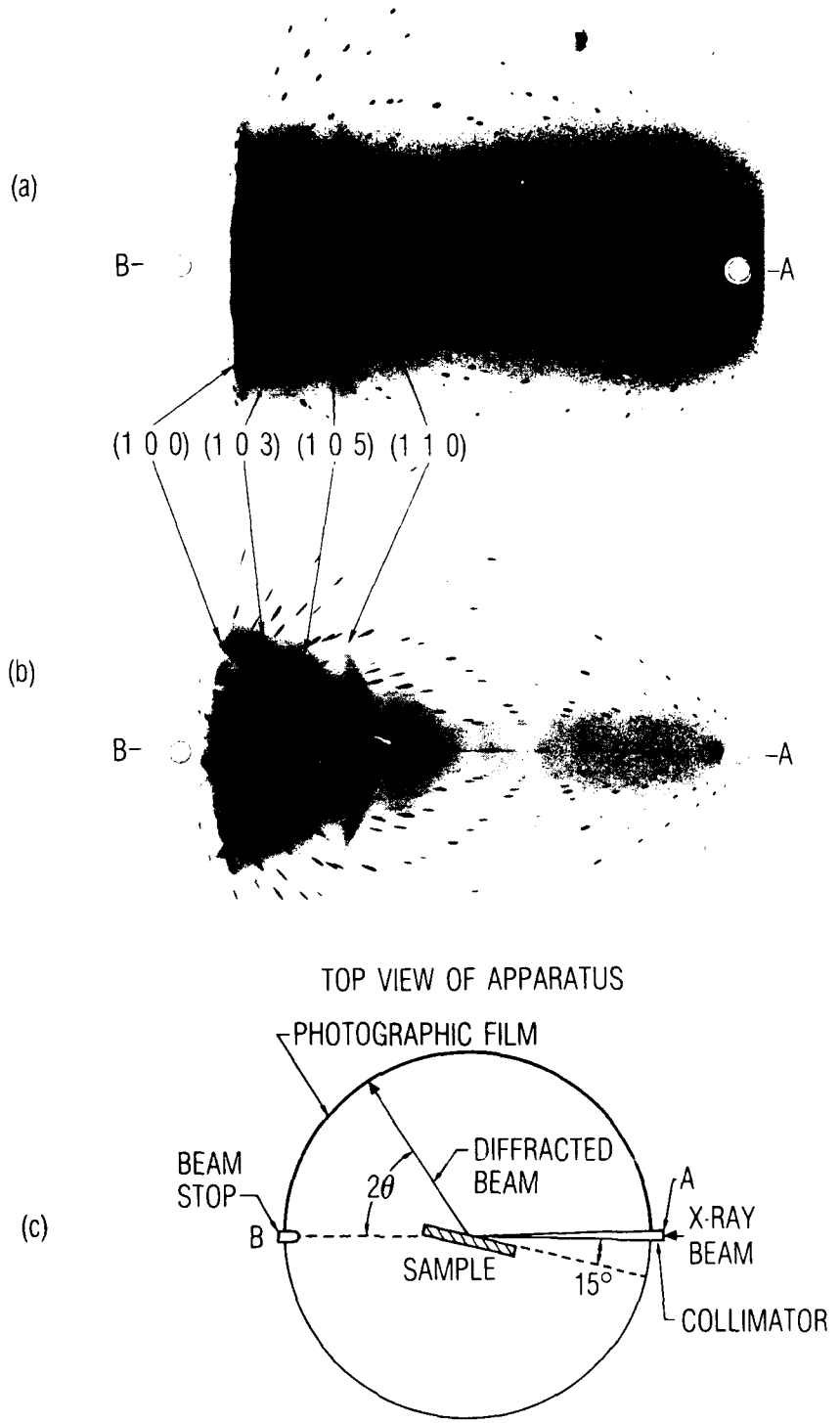

Fig. 6. Read thin-film photographs of a 1-μm-thick MoS_2 film deposited on an oxidized single-crystal silicon substrate held at ~ 70°C during sputtering: (a) taken with a 15° angle of incidence; (b) taken with a 5° angle of incidence. (c) represents the geometry for the Read photo in (a). Points A and B represent the incident and scattered x-ray beams, respectively. The line connecting points A and B in (a) and (b) represents reflections for the plane in the crystallites that is parallel to the substrate surface normal (i.e., perpendicular to the substrate surface).

taken with different x-ray incidence angles to emphasize or de-emphasize the MoS_2 film as compared to the silicon substrate.

The pattern is consistent with the notion that all the crystallites are oriented with (h k 0) planes parallel to the sample surface plane, because no basal plane reflections [i.e., (0 0 l)] are evident in the pattern. The incident x-ray beam is oriented only a few degrees off, but pointing toward, the sample surface [i.e., grazing incidence, see Fig. 6(c)]. If the basal planes are oriented perpendicular to the sample surface, there is no way that the basal planes can contribute to reflections away from the surface onto the film. However, the (1 0 3) and (1 0 5) planes are angled only slightly away from the (0 0 1) plane (i.e., <u>almost</u> normal to the basal planes in the crystallites), and therefore have a possibility of meeting the criterion for reflection away from the surface, which explains the observation of (1 0 3) and (1 0 5) "bands" on the Read photographs. The bands do not cross line A-B, however, because the (1 0 3) and (1 0 5) planes are not oriented far enough from the (0 0 1) plane to enable reflection into the plane perpendicular to the surface.

The presence of the (1 0 0) and (1 1 0) reflections in bands that appear somewhat similar to those for a polycrystalline material suggests that at least several (h k 0) planes have a finite probability of being parallel to the surface normal. For example, if the (1 0 0) planes in all the crystallites were parallel to the surface normal, then the other (h k 0) planes would be able to assume any azimuthal angle with respect to the surface. If the pattern were averaged over all the crystallites, the resulting distribution of angles would produce a band with an apparent polycrystalline structure for all the other (h k 0) directions. The (1 0 0) reflection also would appear as a spot on line A-B, because a fixed x-ray incident direction and a fixed orientation of the (1 0 0) plane would fix the outgoing x-ray direction. In Fig. 6, the intensity of the (1 0 0) band is strongly peaked near line A-B (difficult to see in these photos, but verified in other photos with lower exposure), suggesting that a majority of the crystallites are oriented with their (1 0 0) planes parallel to the substrate surface.

C. X-RAY DIFFRACTION OF MoS_2 FILMS USING THE θ-2θ METHOD

1. ANNEALING OF FILMS SPUTTERED AT AMBIENT TEMPERATURE

The full θ-2θ scan of a 1-μm-thick MoS_2 film sputtered onto a 440C stainless steel substrate is shown in Fig. 7. The peaks due to the MoS_2 film are somewhat diffuse and are labeled with respect to the crystallographic planes they represent. They were positively identified as MoS_2 peaks after comparison with established data on MoS_2[10] and with spectra on stainless steel blank samples and MoS_2 films sputtered on single-crystal silicon and amorphous SiO_2. The few MoS_2-related peaks in Fig. 7, (1 0 0), (1 1 0), and (2 1 0), do not occur at an angle at which stainless steel peaks occur, so their interpretation does not suffer from substrate interference. In our θ-2θ scans, the only reflections in the spectra are for planes oriented parallel to the substrate surface, confirming the results from Sec. III.B that only edge planes [i.e., (h k 0)] are oriented parallel to the substrate surface. Planes (h k l) for which $l \neq 0$ will not appear in the spectra if the standard θ-2θ geometry is used.

The peak widths initially suggest that the crystallites are either very small or exhibit considerable strain, since either effect results in a general symmetric broadening. To examine the crystallinity of the MoS_2 films in more detail, we repeated the scans for several reflections at longer counting times. The spectrum of the (1 0 0) reflection for the as-deposited (nonannealed) sample [Fig. 8(a)] does not exhibit a symmetric, Gaussian shape but appears to be composed of two main peaks at 34.3° and 33.8°, corresponding to d-spacings of 2.61 and 2.65 Å, respectively. The 34.3° peak may be split further into two peaks at 34.2° and 34.5° (2.621 and 2.598 Å). Therefore, the film appears to consist of several types of MoS_2 crystallites, each having a different lattice constant. Each type may exhibit a different crystallite size and degree of strain, but deconvoluting the peaks to obtain their width so that those quantities can be discerned would be difficult because of the proximity of the peaks and the somewhat low signal-to-noise ratio.

The most striking result of the (1 0 0) scan is that the peaks are shifted considerably from the expected (1 0 0) plane spacing of the pure,

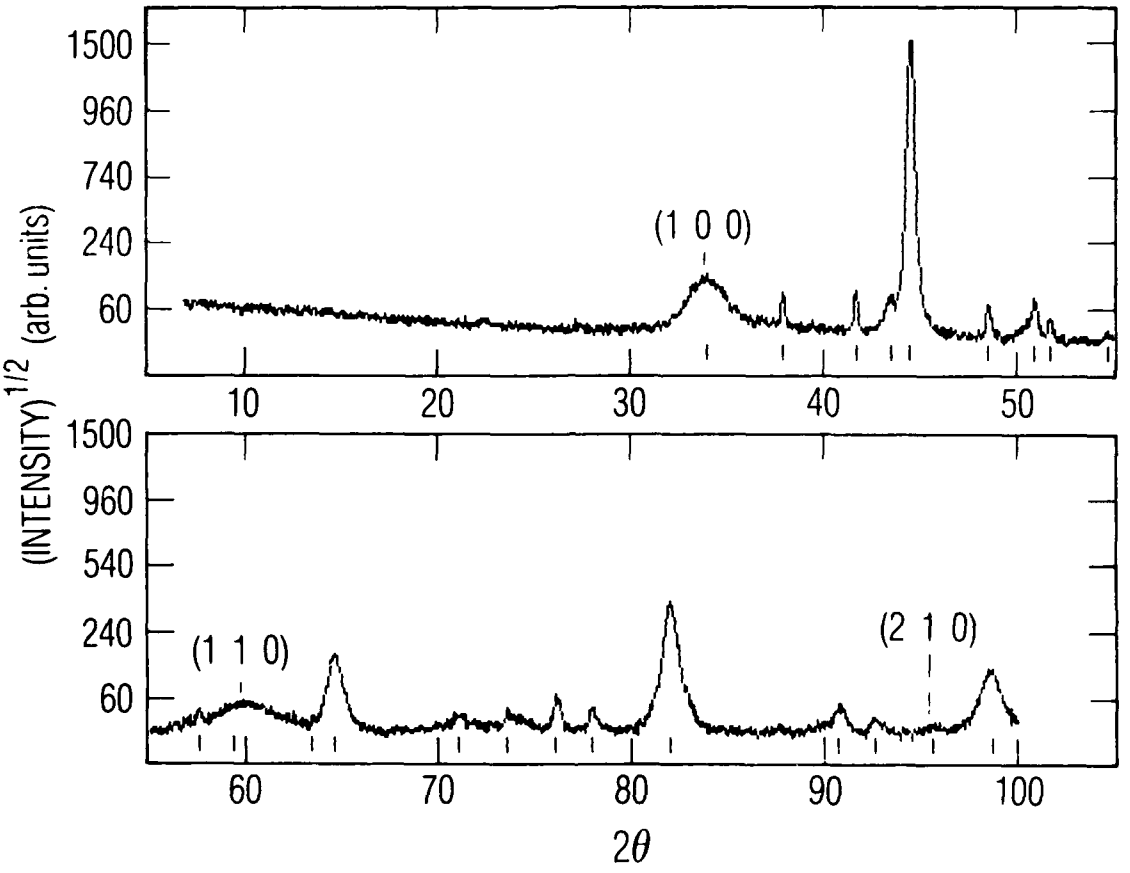

Fig. 7. Full θ-2θ x-ray diffraction scan for a 1-μm-thick AT MoS_2 film deposited on a 440C stainless steel substrate. Labeled peaks are due to MoS_2; remaining peaks are due to the stainless steel substrate.

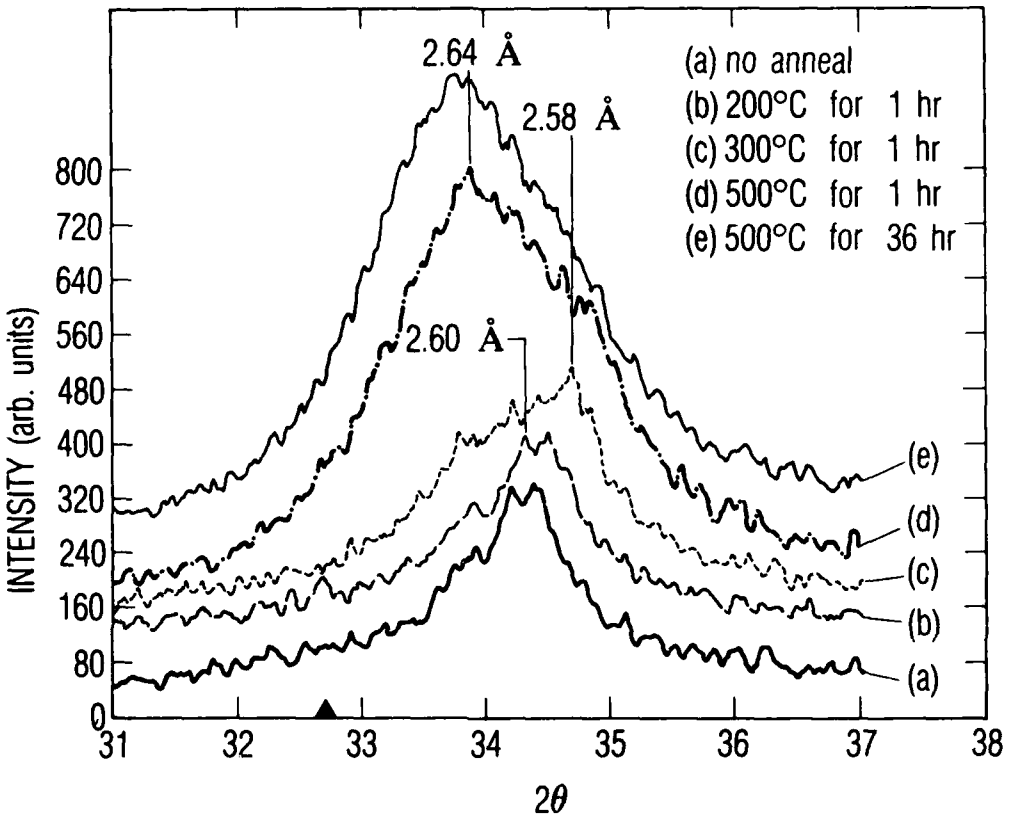

Fig. 8. Scan of the (1 0 0) peak on the AT film using longer counting times for (a) no anneal; for 1-hr anneals at (b) 200°C, (c) 300°C, (d) 500°C; and for (e) a 36-hr anneal at 500°C. Triangle on 2θ axis denotes position of the (1 0 0) peak for a single crystal of molybdenite.

stoichiometric MoS_2 crystal[10] (see Table I). The two peaks in the doublet are shifted by ~ 3% and ~ 5%, representing a considerable compressive stress of the lattice in the (1 0 0) direction. Figure 9 presents the spectrum for the (1 1 0) reflection. Although the lower signal precludes discerning two separate peaks in the samples, the peak also exhibits a smaller (average) (1 1 0) plane spacing than for the molybdenite crystal--a compression of ~ 4% in this case. Therefore, the compression of the as-sputtered MoS_2 films appears to be approximately the same in the directions perpendicular to the various (h k 0) planes. This compression perpendicular to the (h k 0) planes probably occurs along with expansion perpendicular to the (0 0 1) planes (see Sec. III.C.3).

When identical films are annealed to temperatures between 200 and 500°C for 1 hr (followed by cooling to room temperature), two changes in the (1 0 0) peak are observed: (1) The peak at 2.65 Å increases in intensity by as much as 5 times [see Figs. 8(b)-8(d)]; and (2) the peak at 2.61 Å shifts to lower lattice spacing (see Table I) while appearing to gain in intensity only slightly. When the film is annealed at 500°C for longer periods [i.e., 36 hr, see Fig. 8(e)], the 2.61 Å peak seems to disappear almost completely. Upon annealing, the (1 1 0) reflection (see Fig. 9) behaves similarly to the (1 0 0) reflection, as evidenced by the peak's general shifting to higher lattice spacing and increase in intensity. Therefore, annealing appears to partially relieve the stress in the films.

We have confirmed that films can be prepared by sputtering at ambient temperature (AT) that do not exhibit the doublet (1 0 0) structure (see Fig. 10). XPS studies[5] have shown that such films are purer, i.e., have a higher ratio of MoS_2 to oxidized Mo, than the films with the doublet structure: > 90% MoS_2 compared with ~ 70% MoS_2 for those in the present study. The higher purity films are generally produced after extensive operation of the sputtering chamber in the weeks preceding film fabrication, which ensures that the target and the chamber are well outgassed.

The (1 0 0) plane spacing for the higher purity film (see Table I) is 2.65 Å, essentially the same as that for the left-hand (larger lattice

TABLE I. LATTICE SPACINGS IN SPUTTERED MoS_2 FILMS AS DETERMINED BY θ-2θ X-RAY SCANS

Sample	Lattice Spacings (Å) (1 0 0)[a,b] (~34.5°)	(1 1 0)[b] (~ 60.5°)	(0 0 2) (~14°)
MoS_2 crystal	2.737	1.581	6.15
Deposited at ambient temp. (~ 70°C)	(2.598) (2.611) 2.647	1.51	---
Annealed 200°C (1 hr)	(2.604) (2.621) 2.646	1.51	---
Annealed 300°C (1 hr)	(2.584) (2.65)	1.51	---
Annealed 500°C (1 hr)	2.57 2.644	1.54	---
Annealed 500°C (36 hr)	2.647	1.54	---
Higher purity ambient temp. film	2.65	1.54	---
Deposited at high temp. (245°C)	2.621	1.52	---
Ambient temp., worn 10 000 rev	2.61 2.65	1.51	~6.46
High temp., worn 10 000 rev	2.63	1.51	~6.65

[a] The (1 0 0) peak of the AT films generally exhibited a two-peak structure; in the as-deposited and 200°C annealed films, the lower lattice constant peak appeared to be split into two closely spaced peaks, indicated by the parentheses around the lattice constants.

[b] Lattice spacings for (1 0 0) and (1 1 0) peaks have uncertainties of either ±0.003 Å (four significant figures) or ±0.01 Å (three significant figures).

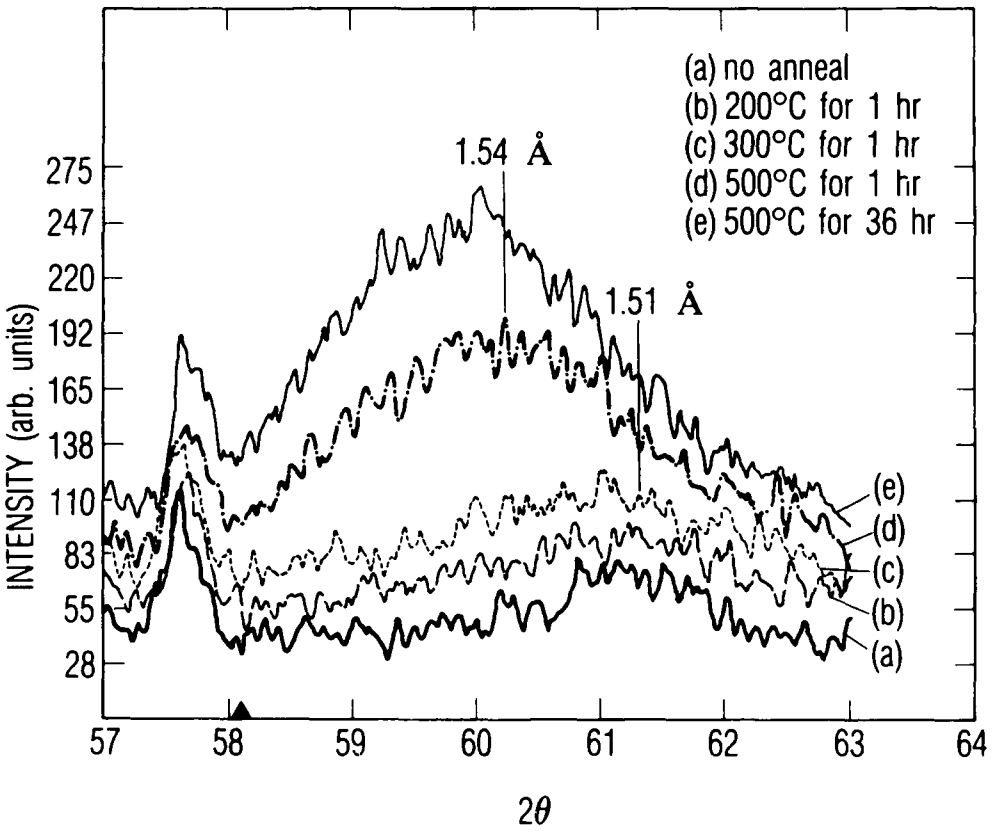

Fig. 9. Scan of the (1 1 0) peak using longer counting times for the same samples as in Fig. 8. The triangle on the 2θ axis denotes the position of the (1 1 0) peak for a single crystal of molybdenite. This triangle is also shown in Fig. 12. The peak at 57.5° is due to the stainless steel substrate.

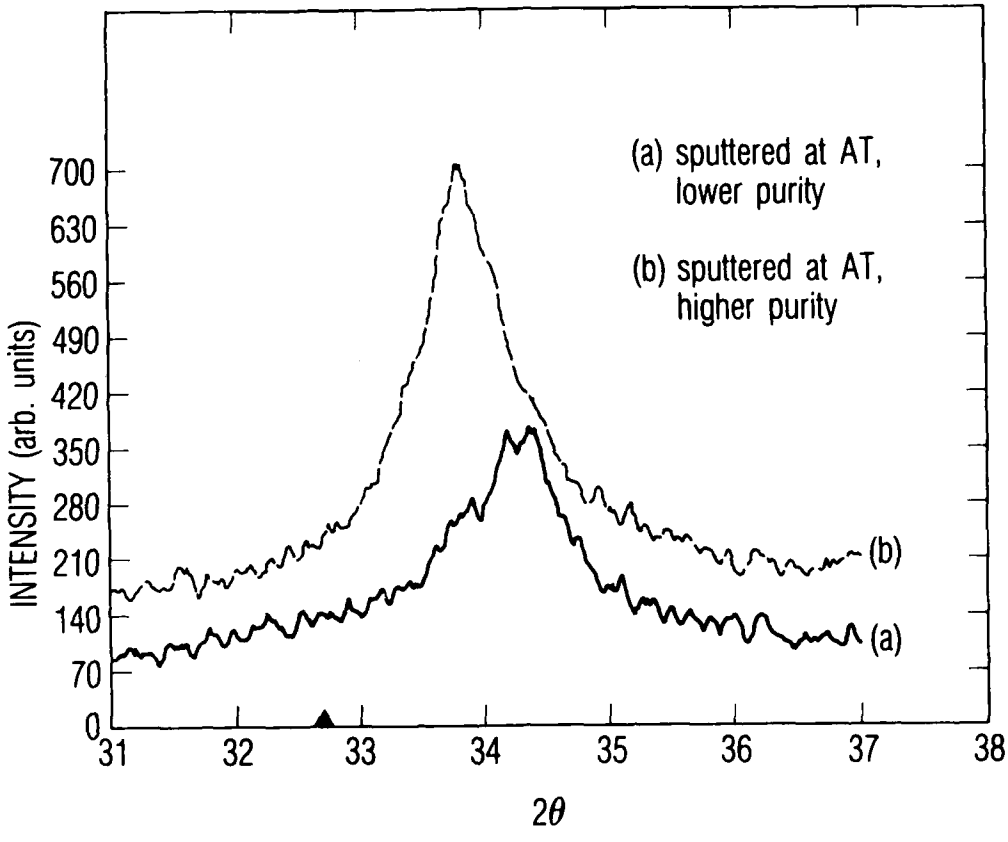

Fig. 10. Comparison of the (1 0 0) peak for (a) a lower purity AT film [same as Fig. 8(a)], and for (b) a higher purity AT film. [Since the two films had different thicknesses, the intensity of the peaks in (a) and (b) should not be compared with each other.] Triangle on 2θ axis denotes position of the (1 0 0) peak for a single crystal of molybdenite.

spacing) peak in the lower purity film (see Fig. 8), which suggests that the smaller lattice spacing peak (2.61 Å) results from impurities substituted into the MoS_2 crystal lattice. As the samples are annealed at increasing temperatures, the larger increase in the higher lattice spacing "pure-film" peak intensity relative to the lower lattice constant "impurity-related" peak intensity probably results from emission of the impurity (probably oxygen) into the vacuum and conversion of the film crystallites to the lower-impurity crystal form. Annealing for extended times [see Figs. 8(e) and 9(e)] appears to reduce the impurity peak intensity to negligible levels.

The presence of impurities in the sputtering chamber is known to cause differences in film morphology: Recent reports have indicated that the presence or absence of H_2O in the sputtering chamber during film growth[11] can explain the difference between type I and type II films.[12] [Type I films are like the films in the present study, whereas type II films have their (0 0 1) planes oriented parallel to the substrate surface.] This study represents the first demonstration of changes in lattice constant in MoS_2 with the level of impurities in the sputtering ambient. Such a clear correlation between the x-ray peak shape and the impurity level in the films suggests that x-ray diffraction can be useful for determining whether an optimal film has been produced on lubricated parts.

2. FILMS SPUTTERED AT ELEVATED TEMPERATURE (~ 245°C)

θ-2θ scans of the (1 0 0) and (1 1 0) reflections were also taken for MoS_2 films that were deposited onto substrates held at 245°C during the sputtering process (designated HT for high-temperature films). The (1 0 0) peaks for AT, annealed (to 500°C for 1 hr), and HT films are shown in Figs. 11(a), 11(b), and 11(c), respectively. The HT peak has less than half the width of, and is also considerably more symmetric than, the others. Its position (2.62 Å) is about midway between that of the impurity-related peak and the pure-film peak in the AT film. Similarly, the position of the (1 1 0) peak for the HT film (1.52 Å) is slightly to the left of the AT (1 1 0) peak (see Fig. 12). Through XPS studies, we have demonstrated that the HT films exhibit very high oxidation resistance;[7] therefore, the position of the (1 0 0) HT peak is unrelated to impurities in the MoS_2 crystal lattice.

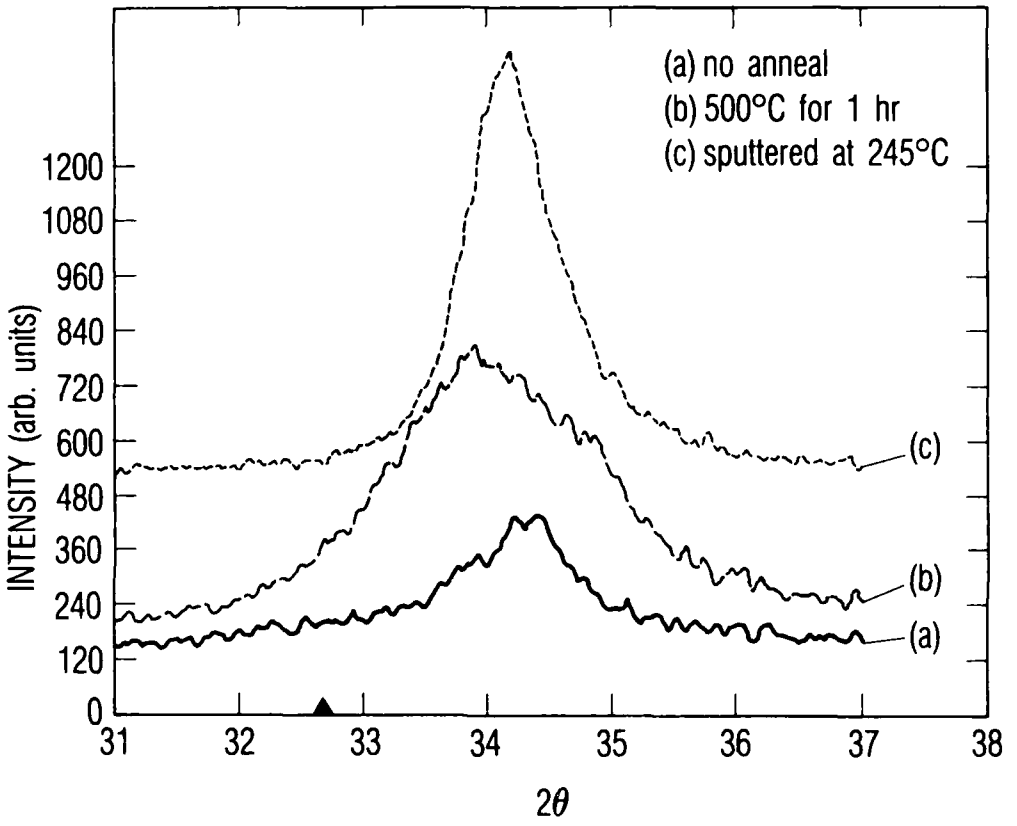

Fig. 11. Scan of the (1 0 0) peak for (a) an AT film with no anneal [same as Fig. 8 (a)], (b) an AT film with an anneal to 500°C for 1 hr [same as Fig. 8(d)], and (c) deposition on a substrate heated to 245°C during sputtering (HT film). Triangle on 2θ axis denotes position of the (1 0 0) peak for a single crystal of molybdenite.

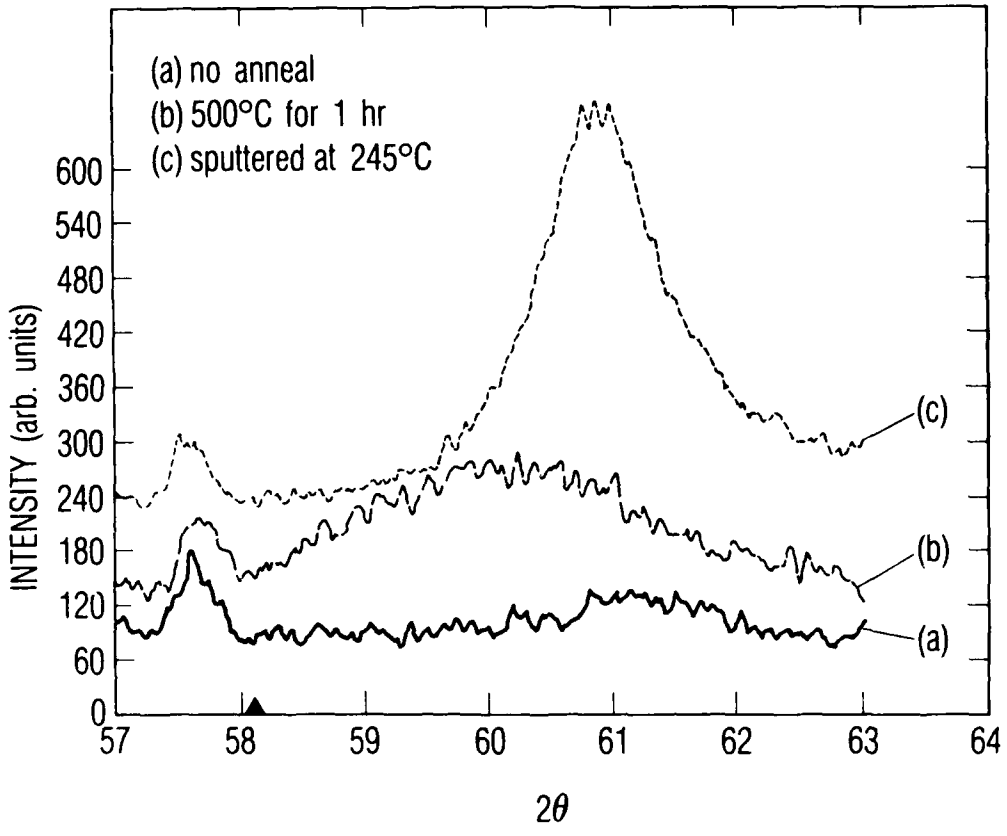

Fig. 12. Scan of the (1 1 0) peak for the same samples as in Fig. 11.

XPS also reveals that the HT films have 3%-7% less sulfur than in stoichiometric MoS_2. Dimigen et al.[4] have shown that sputtered MoS_2 films that are severely deficient in sulfur (~ 50%) still retain the basic MoS_2 crystal structure. Therefore, the sulfur deficiencies are compensated for by a compression in the lattice perpendicular to the (h k 0) planes. Both sulfur deficiencies and oxidation appear to cause compression of the lattice perpendicular to the (h k 0) planes. Such lattice changes can be explained in terms of changes in electron distribution around the Mo atom and are discussed elsewhere.[6]

3. WEAR BEHAVIOR OF FILMS

To determine the effect of the wear process on the various crystalline parameters investigated above, samples of sputtered MoS_2 films were run in the wear testing apparatus described in Sec. II. An AT sample and an HT sample were each subjected to 10 000 rev before being analyzed by x-ray diffraction. That number of revolutions, under identical load conditions, was established in our laboratory as being well below the number required to reach "failure." (Failure was determined arbitrarily to be at a torque of 0.07 N m, which occurred at 3-5 $\times$ 10^5 rev for HT films and 6-12 $\times$ 10^5 rev for AT films.)

The (1 0 0) peaks for the AT and HT films both before and after sliding wear are presented for comparison in Fig. 13. The intensities of both peaks are greatly attenuated after wear, implying that a large portion of the crystallites are reoriented during sliding. The attenuation can probably not be accounted for by a large decrease in the crystallinity of the individual crystallites, because making the crystallites amorphous will cause a large increase in the width of the peaks, which does not seem to be the case. In addition, the positions and structures of the peaks appear to be approximately the same after wear. These observations demonstrate that when the film has been "worn in," but not subjected to extreme wear (i.e., close to failure), the only major change in the crystallinity of the film is the reorientation of its crystallites. A drop in peak intensity was also observed for the (1 1 0) peak (not shown). Therefore, it is probable that all [h k 0] (edge plane) directions are highly reoriented away from the substrate surface normal.

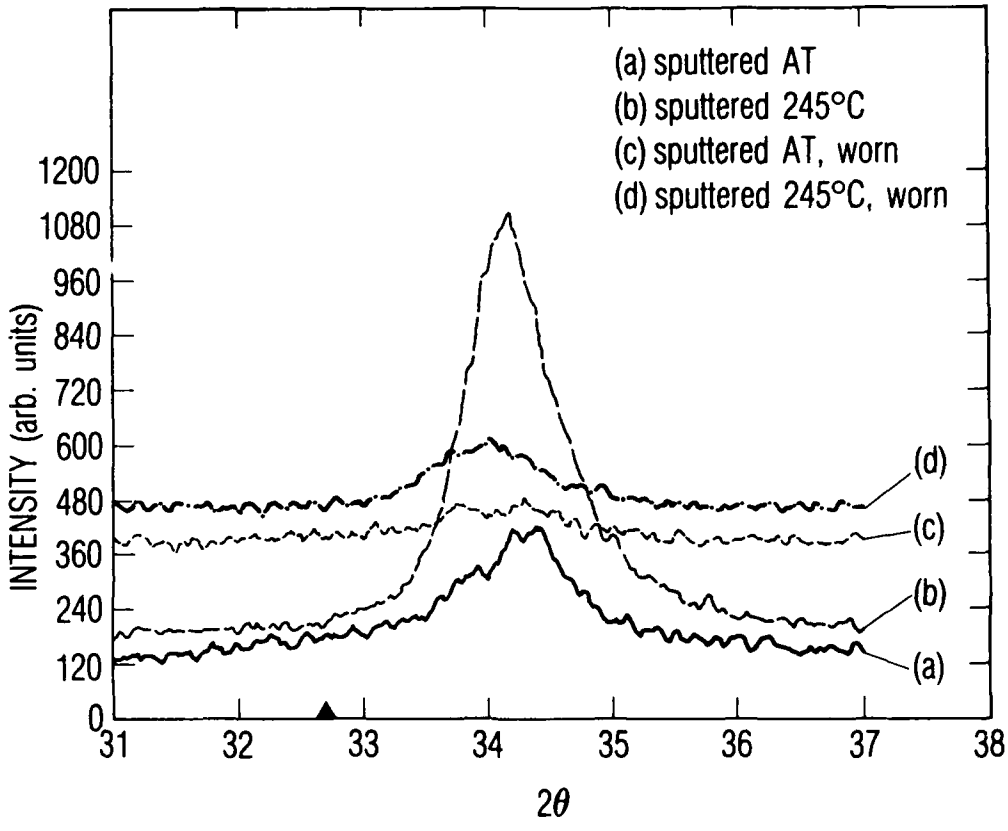

Fig. 13. Scan of the (1 0 0) peak: before wear for (a) the AT film and (b) the HT film [same as Figs. 8(a) and 11(c)]; after 10 000 rev of sliding wear for (c) the AT film and (d) the HT film. With wear, the peak drops considerably for both films, implying a reorientation of the film crystallites. Triangle on 2θ axis denotes position of the (1 0 0) peak for a single crystal of molybdenite.

Scans (θ-2θ) of the region around $2\theta = 14°$ for the worn samples reveal peaks corresponding to the (0 0 2) reflection, which were not observed in unworn samples (see Fig. 14). The appearance of those peaks, along with the disappearance of the (h k 0) peaks for the worn samples, indicates that the crystallites have oriented themselves with their basal planes parallel to the substrate surface plane.

The approximate position of the peak maximum for the (0 0 2) reflection suggests that the lattice is significantly expanded perpendicular to the (0 0 2) plane. The lattice is expanded by ~ 5% for the worn AT film, whereas it is expanded by ~ 8% for the HT film. This expansion (or tensile stress) is probably caused by the same factor that causes compression in the [h k 0] directions: oxygen impurities. The lattice expansion in the [0 0 2] direction may have implications for enhanced lubrication: Jamison[13] reported that a larger distance between basal plane layers results in a decrease in the coefficient of friction.

Studies of the appearance, disappearance, and position of the θ-2θ x-ray peaks with number of wear test revolutions have been conducted in our laboratory for both AT and HT films. The results are reported elsewhere.[14]

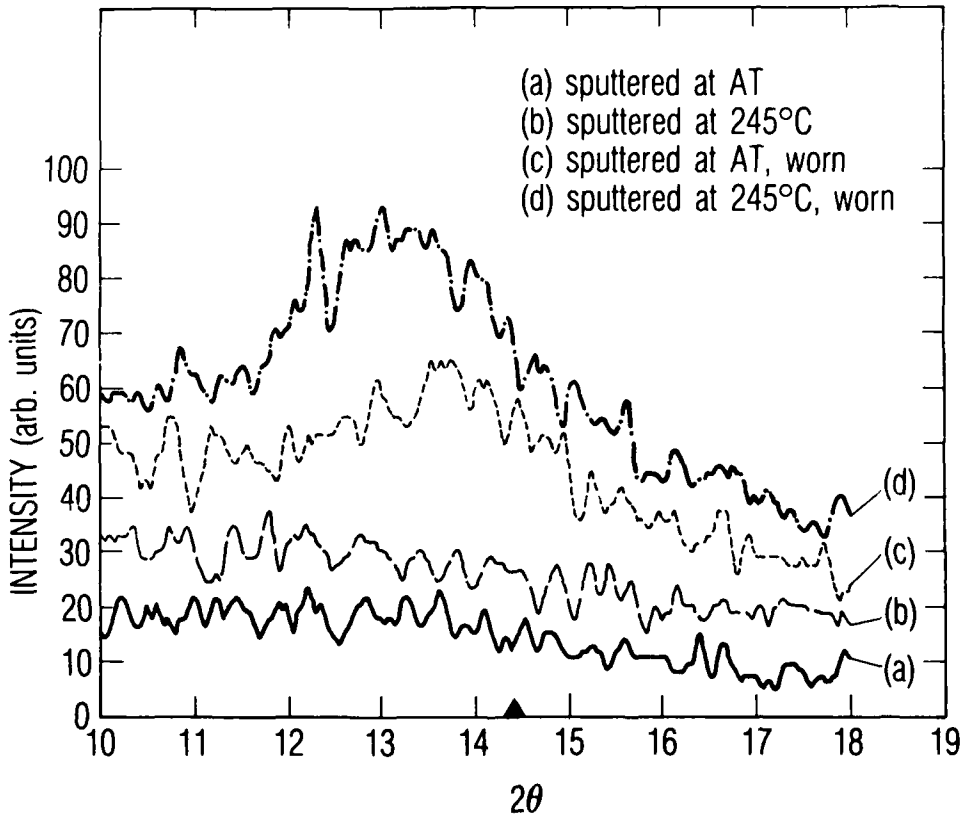

Fig. 14. Scan of the (0 0 2) peak for the same samples as in Fig. 13. The appearance of this peak with wear suggests that the crystallites are reorienting with their basal planes parallel to the substrate surface normal. The triangle on the 2θ axis denotes the position of the (0 0 2) peak for a single crystal of molybdenite.

IV. SUMMARY

X-ray diffraction has been demonstrated to have a number of advantages over transmission electron diffraction: It reveals previously unavailable information on the crystallinity of rf-sputtered MoS_2 films. X-ray diffraction is more versatile than TED, because it can be performed on many different substrates without complex sample-preparation procedures and on films with thicknesses that are the same as for commonly used lubricating films. X-ray line profiles are also obtained more easily, enabling crystalline parameters, such as lattice constant, crystallite orientation, and crystallite size and strain, to be determined more accurately.

Specifically, we have shown that XRD patterns obtained with a Read thin-film camera can provide qualitative information about the crystallite orientation in sputtered MoS_2 films. In the as-deposited films, the crystallites were oriented such that (h k 0) planes were aligned with the substrate surface, whereas the (0 0 1) plane was constrained to be perpendicular to the surface. This observation was corroborated by performing θ-2θ x-ray scans. From detailed analysis of the θ-2θ scans, the lattice in rf-sputtered MoS_2 films was shown to exhibit significant compressive stress perpendicular to the (h k 0) planes for all films studied: The lattice constants in the [h k 0] directions were 3%-5% smaller than for the molybdenite crystal. The (1 0 0) reflections of the higher purity films sputtered on stainless steel substrates that were held at ambient temperature (AT) exhibited single, asymmetric peaks, while AT films with significant oxide formation exhibited a two-peaked structure, the additional peak corresponding to impurity-related effects. As the oxidized AT films were annealed to temperatures as high as 500°C, the intensity of the (1 0 0) peaks increased significantly. However, the intensity of the (1 0 0) peak corresponding to the pure film increased by a factor of ~ 5, whereas the intensity of the (1 0 0) impurity-related peak increased only slightly.

X-ray scans for films deposited on substrates at higher temperatures (HT, i.e., at 245°C) exhibited relatively symmetric (1 0 0) and (1 1 0) peaks that

were more intense and had smaller widths than the peaks for the as-deposited or annealed AT films. The lattice spacing in those directions corresponded to the position of the impurity-related peak in the AT films.

Preliminary studies of the effect of sliding wear on the crystallinity of MoS_2 films have shown that a reorientation of the films' crystallites occurs whereby the basal planes of the crystallites become oriented parallel to the surface normal. Tensile stress was observed in the [0 0 1] direction and may be caused by the compression in the [h k 0] directions.

REFERENCES

1. D. M. Mattox, in Adhesion Measurement of Thin Films, Thick Films, and Bulk Coatings, ASTM special technical publication 640, ed. K. L. Mittal, ASTM, Baltimore, MD (1978), p. 54.

2. O. Nittono, Y. Sadamoto, and S. K. Gong, Jpn. J. Appl. Phys. 26, 157 (1987).

3. T. Spalvins, NASA Tech. Note D-7170 (1973).

4. H. Dimigen, H. Hübsch, P. Willich, and K. Reichelt, Thin Solid Films 129, 79 (1985).

5. N. W. Ashcroft and N. D. Mermin, Solid State Physics, Saunders College, Philadelphia, PA (1976), Chap. 6; see also M. H. Read and C. Altman, Appl. Phys. Lett. 7, 51 (1965).

6. P. D. Fleischauer, in Proceedings of the International Conference Metallurgical Coatings, San Diego, CA, 23-27 March 1987.

7. P. D. Fleischauer and R. Bauer, ASLE Trans. 30, 160 (1987).

8. V. Buck, Vacuum 36, 89 (1986).

9. T. Spalvins, Thin Solid Films 96, 17 (1982).

10. Joint Committee on Powder Diffraction Standards, Powder Diffraction File, Card No. 6-0097, International Center for Diffraction Data, Swarthmore, PA (1980).

11. V. Buck, Thin Solid Films 139, 157 (1986).

12. P. D. Fleischauer, ASLE Trans. 27, 82 (1984).

13. W. E. Jamison, ASLE Trans. 15, 296 (1972); ASLE special publication 14 (1984), pp. 73-87.

14. P. D. Fleischauer and R. Bauer, Trib. Trans. 1, xxx (1988).

END

DATE

FILMED

8-88

DTIC